

Gregory C. Paltakis

Department of Physics, University of Crete, and Research Center of Crete, Heraklion, GR-71003, Greece
(Received April 14, 2024)

The phase fluctuations of the condensate in doped antiferromagnets, described by a $t-t^0$ -J model and a suitable $1/N$ expansion, provide a mechanism for a Kosterlitz-Thouless (KT) type of transition to a superconducting state below T_c . In this paper, we present a Monte Carlo study of the corresponding superfluid weight $D_s(T)$ in the classical (large- N) limit, as a function of temperature and doping. Consistent with generic experimental trends, $D_s(T)$ exhibits a T -linear decrease at low temperatures, with the magnitude of the slope $D_s^0(0)$ increasing upon doping. Finite-size scaling in the underdoped regime predicts values for the dimensionless ratio $A = k_B T_c / D_s(0)$ of order unity, with $A = 0.4435(5)$ in the half-filled band limit, thus confirming $D_s(0)$ as the fundamental energy scale determining T_c . Our Monte Carlo results for $D_s(T) = D_s(0)$ vs $k_B T = D_s(0)$, at 10% hole doping, are found to be in reasonable agreement with recent measurements on $\text{La}_{2-x}\text{Sr}_x\text{CuO}_4$, with $x = 0.10$, throughout the temperature range below the theoretical KT transition temperature T_c .

PACS numbers: 74.40.+k, 74.20.Mn, 74.25.Bt

I. INTRODUCTION

The quest on the nature of the superconducting transition observed in doped antiferromagnets, such as the lamellar high- T_c copper-oxides, has entered a new era. Indeed, a consensus is emerging¹ on the importance of the zero-temperature superfluid weight $D_s(0)$ as the fundamental energy scale determining the corresponding transition temperature T_c . An early clue for this result came from the empirical Uemura relation,² valid for underdoped cuprates, which shows roughly a proportionality between the independently measurable quantities T_c and $D_s(0)$,

$$k_B T_c = A D_s(0); \quad (1)$$

where A is a dimensionless parameter of order unity. Given that the superfluid weight $D_s(T)$, at a general temperature T , measures the "phase stiffness" of the condensate, i.e., the energy cost to produce spatial variations of its phase, Emery and Kivelson³ argued that (1) provides strong evidence for a phase-fluctuation driven superconducting transition. Of course, in strictly two-dimensional systems with continuous $U(1)$ gauge (phase) symmetry, melting of long-range phase coherence with increasing temperature, and hence loss of superfluidity of the charge carriers, proceeds by thermal generation and subsequent unbinding of vortex-antivortex pairs. The detailed description of this transition is given by the Kosterlitz-Thouless (KT) theory^{4,5} in the context of the classical XY model. A characteristic feature of the KT transition is the discontinuous drop of $D_s(T)$ to zero at $T = T_c$, as T_c is approached from below.⁶ Despite the inevitable rounding of this discontinuity by the weak coupling between the copper-oxide layers, Corson et al.,⁷ in a remarkable experiment, have provided direct evidence of the KT nature of the superconducting transition by observing dynamic effects of thermally generated vortices

in the frequency-dependent conductivity of underdoped cuprate thin films.

A common feature of theoretical models⁸⁽¹⁰⁾ assuming a phase-fluctuation mechanism for the superconducting transition, is the prediction of a T -linear decrease in $D_s(T)$ at temperatures well below T_c , in accordance with the experimental observations.^{11;12} However, all the aforementioned models, do not incorporate explicitly the doping dependence of $D_s(T)$ and therefore provide no framework for a proper treatment of the high- T_c cuprate superconductors as doped antiferromagnets. This is a major drawback since the proximity of the doped materials to the Mott insulating antiferromagnetic state at half-filling ($n_e = 1$) leads² to a vanishing $D_s(0)$ and T_c , as the hole concentration ($1 - n_e$) tends to zero. The importance of the antiferromagnetic fluctuations, even well within the underdoped regime, has been recently confirmed in a dramatic way. Specifically, the elastic neutron-scattering measurements³ in pristine $\text{La}_{2-x}\text{Sr}_x\text{CuO}_4$, with $x = 0.10; 0.12$, have established the presence of static long-range antiferromagnetic order in the superconducting ground state, suggested by earlier work.¹⁴ This conclusion is supported also by the subsequent observation of conventional two-magnon Raman scattering¹⁵ in the same material.

The above discussion underlines the need for models of the high- T_c cuprate superconductors that can account, on the same footing, for the intimately coupled phase and spin fluctuations of the condensate. Such a model has been suggested some time ago¹⁶ and shown, by one of the authors, to display flux quantization and a finite superfluid weight, i.e., superconductivity, in its ground state.¹⁷ Our model consists of a $t-t^0$ -J Hamiltonian and a suitable $1/N$ expansion that provide a framework for the study of: (i) the ground-state properties, using standard "spin-wave" techniques which allow the incorporation of leading quantum-fluctuation effects, and (ii) the

finite-temperature properties, using an associated classical (large- N limit) energy functional and corresponding partition function in terms of which important physical quantities can be readily expressed and calculated by Monte Carlo simulation. Point (i) was the subject of earlier works^{16;17} and the results, especially for the optical properties, were found to provide support for our effective model when compared with experiment. In the present paper we consider point (ii), focusing on the study of the superfluid weight as a function of temperature and doping, a subject of current experimental and theoretical interest.

In Sec. II we give a brief description of our effective t - t^0 - J Hamiltonian and the associated classical energy functional and partition function emerging in the large- N limit. In Sec. III we derive an explicit expression for the superfluid weight $D_s(T)$ which we study by Monte Carlo simulation using the standard Metropolis algorithm.¹⁸ We present results for the shape of the scaled curve, $D_s(T)/D_s(0)$ vs $k_B T/D_s(0)$, the value of the dimensionless ratios $k_B T_c/D_s(0)$ and $D_s(T_c)/k_B T_c$, as well as the value of the zero-temperature slope $D_s'(0)$, clarifying their doping dependence in the regime of interest, i.e., close to half-filling. The KT nature of the transition to the superconducting state is supported by finite-size scaling analysis using the relevant Wegner-Minnhagen scaling formula.¹⁹ In particular, our numerical results for the temperature dependence of $D_s(T)$, at 10% hole doping, compare reasonably well with recent measurements¹² in underdoped $\text{La}_{2-x}\text{Sr}_x\text{CuO}_4$, for the corresponding concentration value $x = 0.10$. Furthermore, the zero-temperature slope of the superfluid weight is predicted to approach, close to half-filling ($n_e \rightarrow 1$), the universal value: $D_s'(0) = k_B = 2$, consistent with the available experimental data.^{11;12} The latter limiting value is shown to be a hallmark of the strong antiferromagnetic correlations, present in this temperature and doping regime. Our concluding remarks are summarized in Sec. IV.

II. EFFECTIVE MODEL

The effective model under consideration is described by a t - t^0 - J Hamiltonian expressed in terms of Hubbard operators²⁰ $\hat{O}_{i\alpha}^{ab} = \hat{c}_{i\alpha}^\dagger b c_{i\alpha}^a$ as

$$H = \sum_{ij} t_{ij} \hat{O}_i^0 \hat{O}_j^0 + \frac{1}{2} J \sum_{hi;ji} (\hat{O}_i^+ \hat{O}_j^- + \hat{O}_i^- \hat{O}_j^+); \quad (2)$$

where the index 0 corresponds to a hole, the Greek indices $\alpha, \beta, \gamma, \delta$ assume two distinct values, for a spin-up and a spin-down electron, and the summation convention is invoked. Here J is the antiferromagnetic spin-exchange interaction between nearest-neighbor sites $hi;ji$ on a square lattice endowed with periodic boundary conditions and a total number of sites $N = N_x N_y$, where $N_x = N_y$. For the hopping matrix elements t_{ij} we assume

$$t_{ij} = \begin{cases} t & \text{if } i; j \text{ are nearest neighbors} \\ t^0 & \text{if } i; j \text{ are next nearest neighbors} \\ 0 & \text{otherwise} \end{cases} \quad (3)$$

The conventions in (3) incorporate opposite signs for t and t^0 as it is appropriate for the hole-doped cuprates.²⁰ In Ref. 16 we generalized the local constraint associated with (2) to $\sum_i \hat{O}_i^0 + \hat{O}_i^+ = N$, where N is an arbitrary integer, and considered the commutation properties of the $\hat{O}_{i\alpha}^{ab}$ operators to be those of the generators of the $U(3)$ algebra. A Holstein-Primakoff realization for the latter algebra in terms of hard-core bosons resolves then explicitly the local constraint and can be used to develop a perturbation theory based on the $1/N$ expansion, restoring the physical value $N = 1$ at the end of the calculation.

In the presence of an external magnetic flux, threading the two-dimensional lattice in an Aharonov-Bohm torus geometry, the hopping matrix elements t_{ij} are modified by the well known Peierls phase factor and should be substituted in (2) according to

$$t_{ij} \rightarrow t_{ij} e^{iA_{ij}}; \quad \text{with } A_{ij} = \frac{2}{x} (R_i - R_j) \cdot e; \quad (4)$$

Here R_i is the position vector for lattice site i , e_x is the unit vector along the x -axis encircling the flux lines and $\phi_0 = 2\hbar c/q$ is the so-called flux quantum. As argued in Ref. 17, in the context of the present effective model, whereby carriers are treated as hard-core bosons, the charge q entering ϕ_0 should be set equal to $q = 2e$, where e is the electronic charge.

In the large- N limit "condensation" occurs, i.e., the Bose operators become classical commuting fields. Considering only uniform density configurations, the corresponding classical energy functional resulting from (2) (4) takes the form¹⁷

$$H(\{\}) = \sum_{ij} n_e (1 - n_e) t_{ij} \cos \frac{i}{2} \cos \frac{j}{2} \cos A_{ij} + \frac{i}{2} \frac{j}{2} \frac{i^+}{2} \frac{j}{2} + \sin \frac{i}{2} \sin \frac{j}{2} \cos A_{ij} + \frac{i}{2} \frac{j^+}{2} \frac{i}{2} \frac{j}{2} + \frac{n_e^2}{4} J \sum_{hi;ji} [\cos \alpha_i \cos \alpha_j + \sin \alpha_i \sin \alpha_j \cos(\alpha_i - \alpha_j)] \quad (5)$$

where n_e is the average electronic density, the angles $(\alpha_i; \alpha_j)$ determine the local spin direction, and the remaining parameter α_i determines the local phase of the condensate. The above functional form makes apparent the coupling between the phase and spin variables of the condensate through the kinetic energy term, proportional to t_{ij} .

The description of the finite-temperature classical theory is now completed using the energy functional (5) to

construct the corresponding partition function $Z(\beta)$ and free energy per lattice site $F(\beta)$,

$$Z(\beta) = e^{-\beta F(\beta)} = \int \prod_i d\mathbf{R}_i d\mathbf{R}_{i+\mathbf{e}_x} d\mathbf{R}_{i+\mathbf{e}_y} d\mathbf{R}_{i+\mathbf{e}_x+\mathbf{e}_y} e^{-\beta H(\beta)}; \quad (6)$$

where $\beta = 1/(k_B T)$ and the integrations at each lattice site i extend over the intervals: $0 \leq R_{ix} \leq 2\pi$, $0 \leq R_{iy} \leq 4\pi$. Invoking standard thermodynamic identities, important physical quantities can be readily expressed in terms of the partition function (6) and studied by Monte Carlo simulation. In the following we focus our discussion on the study of the superfluid weight $D_s(T)$.

III. SUPERFLUID WEIGHT

At a finite temperature T , the superfluid weight (or helicity modulus) $D_s(T)$ is given by the curvature of the finite lattice limit of the free energy $F(\beta)$ at $\beta \rightarrow \infty$,^{21,23}

$$D_s(T) = -\frac{1}{2} \frac{\partial^2 F(\beta)}{\partial \theta^2} \Big|_{\theta=0}; \quad (7)$$

Physically, $D_s(T)$ determines the ratio of the density of the superfluid charge carriers to their mass and hence can be related to the experimentally measurable in-plane magnetic (London) penetration depth, as noted later on in this section. Carrying out the second derivative with respect to θ in (7) we have more explicitly that

$$D_s(T) = n_e(1-n_e) \frac{2}{z} \sum_{i,j}^* t_{ij}^2 \mathcal{R}_i \cdot \mathcal{R}_j^2 + \cos \frac{i}{2} \cos \frac{j}{2} \cos \frac{i+j+i+j}{2} + \sin \frac{i}{2} \sin \frac{j}{2} \cos \frac{i+j+i+j}{2} + [n_e(1-n_e)]^2 - \sum_{i,j}^* t_{ij}^2 [(R_i - R_j) \cdot \mathbf{e}_i] \cos \frac{i}{2} \cos \frac{j}{2} \sin \frac{i+j+i+j}{2} + \sin \frac{i}{2} \sin \frac{j}{2} \sin \frac{i+j+i+j}{2}; \quad (8)$$

$z = 4$ being the coordination number of the square lattice. As shown in Ref. 16, close to half-filling ($n_e < 1$) and for a sufficiently large t^0 , the ground state of (5), in the absence of magnetic flux ($\phi = 0$), is described by a

planar spin configuration ($\phi_i = \phi = 2$) in which the local twist angles and phases exhibit long-range order according to: $\phi_i = Q \cdot \mathbf{R}_i$, $\phi_i = Q^0 \cdot \mathbf{R}_i$, where $Q = (\pi; \pi)$ is the usual spin-modulating antiferromagnetic wavevector and $Q^0 = (\pi; 0)$ is a phase-modulating wavevector. The zero-temperature value of the superfluid weight follows then easily from (8) as

$$D_s(0) = 4t^0 n_e (1 - n_e); \quad (9)$$

For the typical two-dimensional model with continuous symmetry under consideration, we expect that at low but finite temperatures, the long-range order will be destroyed by the proliferation of excited Goldstone modes, leading to a T -linear decrease of $D_s(T)$. At higher temperatures we expect that the thermal generation and subsequent unbinding of vortex-antivortex pairs will lead eventually to a discontinuous drop of $D_s(T)$ to zero, at a critical point $T = T_c$, in a KT type of transition. In order to study numerically $D_s(T)$ in the whole temperature range and attain the aforementioned physical picture, we performed a Monte Carlo simulation using the standard Metropolis algorithm.¹⁸ Our calculations were carried out on small lattices, with typical sizes $L_x = 8; 16; 32; 64$. For a given temperature we performed of the order of 10^4 thermalization steps and of the order of 10^6 measurements. We considered values for the dimensionless ratios $t^0/t = 0.45$ and $t/J = 1.0$, which are thought to be relevant for the copper-oxide layers, and restricted our study to the underdoped regime, i.e., to small $(1 - n_e)$ values up to 10% hole doping. The latter restriction is dictated by the fact that models of the t^0 - J kind, being rather simple extensions of the Motz-Hohenberg antiferromagnetic insulator, cannot properly account for the nontrivial evolution of the electronic structure of the cuprates that occurs at higher doping values, namely, the closing of the pseudogap²⁴ in the optimally doped and overdoped (Fermi liquid) regime.

Typical Monte Carlo results for the superfluid weight vs temperature are shown in Fig. 1 (a), for $(1 - n_e) = 0.01$, and Fig. 1 (b), for $(1 - n_e) = 0.10$. At low temperatures the superfluid weight has a weak finite-size dependence and displays the expected T -linear decrease. In particular, for $T \neq 0$ and $n_e \neq 1$, we have established the asymptotic form

$$\frac{D_s(T)}{D_s(0)} = 1 - \frac{k_B T}{2D_s(0)} \quad \text{for } T \neq 0 \text{ and } n_e \neq 1; \quad (10)$$

The analytic expression (10) is shown in Fig. 1 by a dotted line. Evidently, this asymptotic line is approached very closely from below by the low temperature numerical data already in the case of the 1% hole doping; see Fig. 1 (a). From (10) follows that the zero-temperature slope of the superfluid weight approaches, close to half-filling, the parameter-free universal value:

$$D_s^0(0) = k_B^{-1} = 0.043 \text{ meV K}^{-1} \quad \text{for } n_e \neq 1; \quad (11)$$

The upper limiting value (11) is a rather stringent prediction of our theory and seems, indeed, to be consistent with the available experimental data^{11;12} in the high- T_c cuprate superconductors. A comparison of Fig. 1 (a) with Fig. 1 (b) reveals an increase in the magnitude of the slope $D_s^0(0)$ upon doping, a trend also consistent with experiment.^{11;12}

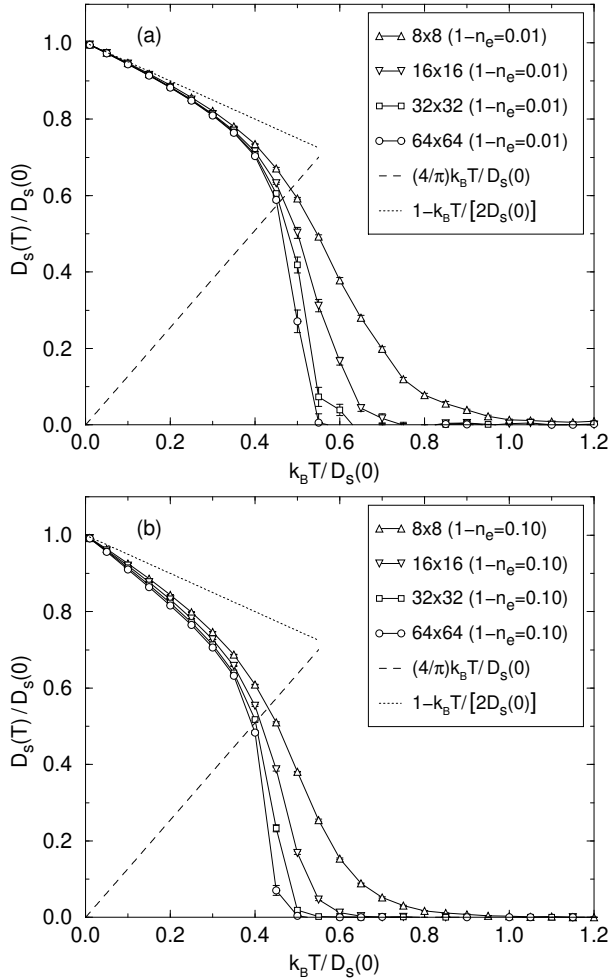


FIG. 1. Superfluid weight $D_s(T)$ vs temperature, for various lattice sizes, $t = 4.5$, $t = J = 1.0$, and (a) $1 - n_e = 0.01$ [estimated $k_B T_c = D_s(0) = 0.4346(9)$], (b) $1 - n_e = 0.10$ [estimated $k_B T_c = D_s(0) = 0.3502(8)$]. Monte Carlo points above the corresponding estimated KT transition temperature T_c are nonzero due to finite-size effects. Error bars are included but in most cases are smaller than symbol size.

We emphasize that the asymptotic form (10) is a physical consequence of the fact that close to half-filling the antiferromagnetic exchange energy, Jn_e^2 , overwhelms the hole kinetic energy, $t_{ij}n_e(1 - n_e)$, and in particular the term $D_s(0)$ given by (9). Hence, in the limit $n_e \rightarrow 1$ and in the relevant temperature range $k_B T \ll D_s(0) \ll Jn_e^2$ (so that $T \rightarrow 0$), the thermal average (8) may be simplified by freezing the spin variables ($s_i; s_j$) to their zero-temperature antiferromagnetic configuration and allowing fluctuations only in the phase variables ϕ_i . In this

case, the vanishing overlap between the opposite sublattice spin states leaves the direct hopping t^0 between next-nearest-neighbor (n.n.n) sites as the only relevant process of charge transport. One can then easily show that the expressions for the energy functional (5) and superfluid weight (8) reduce to those of a classical XY model for the ϕ_i variables, but with only a n.n.n interaction I , where $I = D_s(0)/2$. The reduction of the structure of the phase fluctuations, close to half-filling, to that of the n.n.n XY model and not to the commonly assumed^{3;17;25} structure of the nearest-neighbor (n.n) XY model, is an important prediction and a direct consequence, in the context of our theory, of the presence of strong antiferromagnetic correlations in this regime. Numerically, the validity of our argument becomes apparent in Fig. 2 displaying almost coinciding $D_s(T)$ Monte Carlo data for the n.n.n XY model (opaque diamonds) and the $t-t^0$ -J model with a very small hole concentration ($1 - n_e = 0.01$) (filled diamonds). Therefore, we may exploit the detailed results of Appendix A for the n.n.n XY model, see Eq. (A 5), to conclude the asymptotic form (10) and hence the limiting value (11). The latter value, $D_s^0(0) = k_B = 2$, being twice that of the n.n XY model (see Appendix A), serves as a distinct hallmark of the sublattice structure of the strong antiferromagnetic correlations in the limit $n_e \rightarrow 1$. Our observations here are also, by analogy to the well-known physics of the XY model, the presence of a KT transition for the superfluid weight of the $t-t^0$ -J model, when $n_e \rightarrow 1$, and allow to transcribe relevant results for the former model, established in Appendix A, to the latter, e.g.,

$$\frac{D_s(T_c)}{k_B T_c} = \frac{4}{\pi} \quad \text{for } n_e \rightarrow 1; \quad (12)$$

$$k_B T_c = D_s(0) = 0.4435(5) \quad \text{for } n_e \rightarrow 1; \quad (13)$$

In Fig. 1 and Fig. 2 we present $(4/\pi)k_B T = D_s(0)$ by a short dashed line. According to (12), in the limit $n_e \rightarrow 1$ the latter line should intersect the corresponding Monte Carlo data curve of $D_s(T) = D_s(0)$ vs $k_B T = D_s(0)$ precisely at the $k_B T_c = D_s(0)$ value given by (13); see opaque (filled) diamonds in Fig. 2.

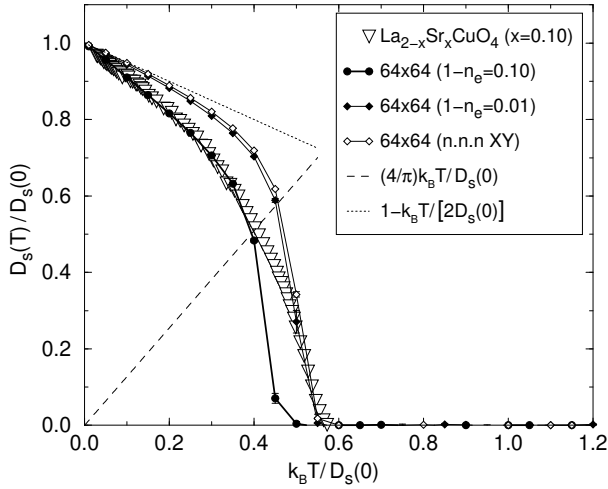


FIG. 2. Superfluid weight $D_s(T)$ vs temperature. Experimental data (triangles) on $\text{La}_{2-x}\text{Sr}_x\text{CuO}_4$ ($x=0.10$), are extracted from the measurements of Panagopoulos et al.¹² using Eq. (15). Corresponding Monte Carlo results (circles) are calculated for lattice size 64×64 and $\mu = 0.45$, $t=J = 1.0$, $1 - n_e = 0.10$. Also included are results for the same lattice size and $\mu = 0.45$, $t=J = 1.0$, $1 - n_e = 0.01$ (filled diamonds), which should be compared with the results for the $n.n.n$ XY model (opaque diamonds). The latter model corresponds to the limiting form of the present $t-t^0$ -J model, when $n_e \neq 1$, as discussed in the text.

It should be noted that in the actual simulations of the $t-t^0$ -J model we can only use finite, though possibly small, hole concentrations which inevitably lead to deviations from the limiting values (12)–(13). In order to obtain rather accurately the corresponding transition temperature T_c we have used the finite-size scaling analysis of Weber and Mühnchen,¹⁹ which is appropriate for KT type of transitions. In this analysis one measures the chi-square values $\chi^2(T)$ of the fitting of the Monte Carlo data for the superfluid weight, at each given temperature and for a sequence of small lattice sizes, to a certain scaling formula, derived by the latter authors from the Kosterlitz renormalization group equations.²⁶ Specifically, one assumes at each temperature T the following x -dependence of the superfluid weight $D_s(T; x)$,

$$\frac{D_s(T; x)}{2k_B T} = R(T) \left[1 + \frac{1}{2 \ln[x = \xi_0(T)]} \right]; \quad (14)$$

where $\xi_0(T)$ is some characteristic length of the order of the lattice constant and has no singularity at $T = T_c$. The logarithmic lattice size dependence involved in (14) is characteristic of the presence of vortices in the KT transition. Strictly speaking (14) is correct only at the critical point $T = T_c$. Given now a value for $R(T_c)$, the critical temperature can be determined by two alternative procedures: (a) we expect $R(T)$ to be $R(T_c)$ and use $\xi_0(T)$ as the only adjustable parameter in (14) to measure the chi-square values $\chi^2(T)$ of the fitting, in which case T_c corresponds to the minimum of the $\chi^2(T)$ curve, or (b) we use both $R(T)$ and $\xi_0(T)$ as adjustable param-

eters in (14) and determine T_c from the point where the $R(T)$ curve crosses the line $R(T) = R(T_c)$. The correct value for $R(T_c)$ should lead uniquely to the same value for T_c in both procedures. The application of this finite-size scaling to the $n.n.n$ XY model is summarized pictorially in Fig. 4 of Appendix A and justifies, as far as the $t-t^0$ -J model is concerned, the limiting values (12)–(13) with $R(T_c) \neq 2$, for $n_e \neq 1$.

For the finite doping value $(1 - n_e) = 0.01$ or $(1 - n_e) = 0.10$ (and fixed $\mu = t-t^0 = 0.45$, $t=J = 1.0$), the application of the aforementioned finite-size scaling analysis, using the lattice size sequence $x = 4; 6; 8; 10; 12$, leads to: $k_B T_c/D_s(0) = 0.4346(9)$ with $R(T_c) = 2.04$, or $k_B T_c/D_s(0) = 0.3502(8)$ with $R(T_c) = 2.51$, respectively. To be sure, the presence in Fig. 1 of non-zero $D_s(T)$ values above the corresponding T_c , instead of a discontinuous drop to zero, is due to finite-size effects which grow rapidly above the estimated critical temperature; a typical behavior for a KT transition. Indeed, following an original argument by Weber and Mühnchen,¹⁹ we note that the success of the scaling formula (14) in the present model provides, ipso facto, strong evidence that the relevant phase transition is of the KT type. Our results show a modest increase of the jump ratio $D_s(T_c)/(k_B T_c) = 2R(T_c) =$ upon doping. The latter behavior seems physically similar to that known in the literature of the frustrated XY model^{27;28} given that, in the context of the $t-t^0$ -J model, doping induces a form of dynamic frustration for the phase variables, via their inevitable coupling to the fluctuating spin variables.

Furthermore, our results show that the dimensionless parameter $A = k_B T_c/D_s(0)$, introduced in context of the empirical Uemura relation (1), is not doping independent but decreases modestly upon doping, while away from half-filling it also depends on the couplings μ and $t=J$. Nevertheless, for rough theoretical estimates of the KT transition temperature T_c in terms of $D_s(0)$, in the underdoped regime, one may always use the universal limiting value $A = 0.4435(5)$, for $n_e \neq 1$, quoted in (13). We remind that that the latter value is characteristic of the $n.n.n$ XY model and equals to half the corresponding value of the $n.n$ XY model (see Appendix A) commonly employed to this end.^{3;17;25} Note that the use of $A = 0.4435(5)$ in conjunction with (1) brings earlier theoretical overestimations of the KT transition temperature for the copper-oxides layers,^{17;25} derived with $A \approx 0.9$, down to more reasonable values. In all cases, the present analysis confirms $D_s(0)$ as the fundamental energy scale determining T_c in the underdoped regime.

Having discussed the generic trends of the superfluid weight as a function of temperature and doping, in the underdoped regime, it is instructive to provide a more direct comparison of our theory with experiment. To this end we note that in the lamellar high- T_c superconductors, the experimental value for the superfluid weight per copper-oxide plane, $D_s^{(\text{exp})}(T)$, can be extracted from the directly measurable^{11;12} in-plane magnetic (London)

penetration depth, $\lambda_{ab}(T)$, using the relation:^{3,10,25}

$$D_s^{(exp)}(T) = \frac{(hc)^2 d}{4 q^2 \lambda_{ab}^2(T)}; \quad (15)$$

where d is the average distance between planes and we remind that $q = 2e$. Using the experimental data of Panagopoulos et al.¹² for $\lambda_{ab}(T)$ on the underdoped $\text{La}_{2-x}\text{Sr}_x\text{CuO}_4$, with $x = 0.10$, and the structural parameter²⁹ $d = 6.64 \text{ \AA}$, we depict in Fig. 2 by triangles the corresponding experimental values (15) for the superfluid weight vs temperature. As a result of the weak coupling between the copper-oxide layers, the experimental data display no KT discontinuity but rather a continuous drop of the superfluid weight to zero, at a specific temperature value, that is not simply related to the ideal KT transition temperature of a copper-oxide monolayer. Corresponding Monte Carlo results for 10% hole doping are depicted in Fig. 2 by circles and calculated for a 64×64 lattice, with $\beta = 0.45$ and $t=J = 1.0$. As noted earlier in this section, the theoretical KT transition temperature for the latter set of parameters is $k_B T_c = D_s(0) = 0.3502(8)$, while nonzero Monte Carlo points above this value are due to finite-size effects. Evidently, our theoretical results (circles) in Fig. 2 compare reasonably well with the experimental data (triangles) throughout their common relevant temperature range, i.e., up to T_c .

In Fig. 2 we also depict Monte Carlo results for 1% hole doping (filled diamonds), as well as results for the $n.n.n$ XY model (opaque diamonds), thus providing the theoretical lineshape of the superfluid weight vs temperature, in the limit $n_e \rightarrow 1$. Clearly, it will be very interesting to have measurements of the in-plane magnetic penetration depth on $\text{La}_{2-x}\text{Sr}_x\text{CuO}_4$, with hole concentration x as small as it is experimentally possible, to compare with the present definite theoretical prediction.

IV. CONCLUDING REMARKS

In this paper we have presented a study of the temperature and doping dependence of the superfluid weight $D_s(T)$ in doped antiferromagnets described by the $t-t^{\prime}$ - J model (2)–(3). Using Monte Carlo simulations and finite-size scaling analysis we have demonstrated that the phase transitions of the condensate, emerging in an appropriate classical (large- N) limit, drive superconductivity via a Kosterlitz-Thouless type of transition. Our theoretical results reproduce important generic experimental trends of $D_s(T)$, observed in the underdoped high- T_c cuprate superconductors. This includes the T -linear decrease of $D_s(T)$ at low temperatures and the increase of the magnitude of the slope $D_s^{\prime}(0)$ upon doping.

In particular, the sublattice structure of the strong antiferromagnetic correlations in the half-filled band limit was shown to dictate the lineshape of $D_s(T) = D_s(0)$ vs $k_B T = D_s(0)$, for $n_e \rightarrow 1$, to be identical to that of the

$n.n.n$ XY model. In order to check this definite theoretical prediction we have suggested measurements of the in-plane magnetic penetration depth in very lightly doped cuprates. Here we should add that higher order $1=N$ corrections are expected to renormalize downwards¹⁷ the fundamental energy scale $D_s(0)$ but, nevertheless, leave the lineshape of the scaled curve $D_s(T) = D_s(0)$ vs $k_B T = D_s(0)$ essentially intact.

The present study shares some common features with earlier works^{8,10} invoking a phase-fluctuation mechanism for the high- T_c superconductivity. On the other hand, all these works including ours are radically different from phenomenological approaches^{30,31} that implicate the thermally excited nodal quasiparticles in a d -wave BCS superconducting state for the reduction of $D_s(T)$ with increasing temperature. The weak-coupling BCS type of approaches, however, are undermined by the absence of normal state quasiparticle peaks³² near the Brillouin zone points $(0; \pi)$ and $(\pi; 0)$ where superconductivity is supposed to originate. At present it is still difficult to discern experimentally whether the temperature and doping dependence of $D_s(T)$ is dominated by phase fluctuations or by nodal BCS-like quasiparticle excitations. However, recent experiments in cuprate thin

films have provided strong evidence for the inherent two-dimensional character of superconductivity³³ and for the KT nature of the superconducting transition⁷.

ACKNOWLEDGMENTS

I would like to thank C. Panagopoulos for providing the penetration depth data and X. Zotos and G. Varelogiannis for stimulating discussions.

APPENDIX A: GENERALIZED XY MODEL

In the main body of the paper we noted that the structure of the phase fluctuations of the $t-t^{\prime}$ - J model under study reduces, in the half-filled band limit, to that of a classical XY model with only next-nearest-neighbor ($n.n.n$) interactions. In order to clarify the properties of the latter model, in juxtaposition to those of the more conventional nearest-neighbor ($n.n$) XY model, we consider briefly in this appendix the following Hamiltonian

$$H_{XY} = \frac{1}{2} \sum_{i,j} X_{ij} \cos(\theta_i - \theta_j); \quad (A1)$$

assuming

$$X_{ij} = \begin{cases} 8 & \text{if } i, j \text{ are nearest neighbors} \\ 1 & \text{if } i, j \text{ are next nearest neighbors} \\ 0 & \text{otherwise;} \end{cases} \quad (A2)$$

where θ is a free parameter, with $0 \leq \theta \leq \pi$, and $I > 0$. At each lattice site i the angle θ_i varies in the interval: $0 \leq \theta_i \leq 2\pi$. Evidently, $\theta = 0$ corresponds to the n.n XY model, while $\theta = \pi$ corresponds to the n.n.n XY model.

The superfluid weight (or helicity modulus) for the generalized XY model (A 1) reads

$$D_s(T) = \frac{2}{z} \sum_{\langle ij \rangle} \frac{1}{2} \left[\mathcal{R}_i \mathcal{R}_j \cos(\theta_i - \theta_j) - \frac{1}{2} \sum_{\langle ij \rangle} \mathcal{I}_{ij} [(\mathcal{R}_i - \mathcal{R}_j) \sin(\theta_i - \theta_j)] \right]; \quad (A 3)$$

in agreement with corresponding early results.²⁷ In view of (A 2), the ground state configuration of (A 1) is simply given by $\theta_i = 0$, while the zero-temperature value of the superfluid weight follows immediately from (A 3) as

$$D_s(0) = (1 + I)I; \quad (A 4)$$

Integrating the quadratic (Gaussian) fluctuations around the ground state configuration we obtain, after some lengthy algebra, the following low-temperature asymptotic expansion for the superfluid weight

$$\frac{D_s(T)}{D_s(0)} = 1 - \frac{1}{2} G(\theta) \frac{k_B T}{z D_s(0)} \quad \text{for } T \ll 0; \quad (A 5)$$

Here $G(\theta)$ is a dimensionless geometric factor given by

$$G(\theta) = \frac{1}{q} \frac{(1 - \cos \theta)}{(1 - \cos \theta) + (1 - \cos \theta)}; \quad (A 6)$$

with

$$q = \frac{1}{2} (\cos \theta_x + \cos \theta_y); \quad \theta_x = \cos \theta_x \cos \theta_y; \quad (A 7)$$

We emphasize that $G(\theta)$ is an increasing function of θ with end-point values: $G(0) = 0$ and $G(\pi) = 1$. Hence, from (A 5) follows that the zero-temperature slope $D_s^0(0)$ evolves monotonically from $k_B T_c = 4$ to $k_B T_c = 2$, as the parameter θ varies from 0 (n.n XY model) to π (n.n.n XY model); see dash-dotted and dotted lines in Fig. 3.

Noting now that $\mathcal{R}_i \mathcal{R}_j = 2$, for n.n.n sites i, j , whereas $\mathcal{R}_i \mathcal{R}_j = 1$, for n.n sites i, j , a cautious inspection of (A 3) reveals that, in the thermodynamic limit and at each given temperature T , the superfluid weight of the n.n.n XY model should be twice as large the superfluid weight of the n.n XY model: $D_s^{(=1)}(T) = 2D_s^{(=0)}(T)$. The latter property is explicit in the low-temperature analytic results (A 4)–(A 5) and we have confirmed its validity in the whole temperature range by Monte Carlo simulation using the standard Metropolis algorithm with the parameters quoted in Sec. III. Indeed, as shown in Fig. 3, the Monte Carlo data curves of

$D_s(T) = D_s(0) \text{ vs } k_B T = D_s(0)$ for the n.n.n XY model coincide, within numerical error, with those for the n.n XY model, when the $k_B T = D_s(0)$ axis is scaled by a factor of 2. This agreement becomes better with increasing lattice size.

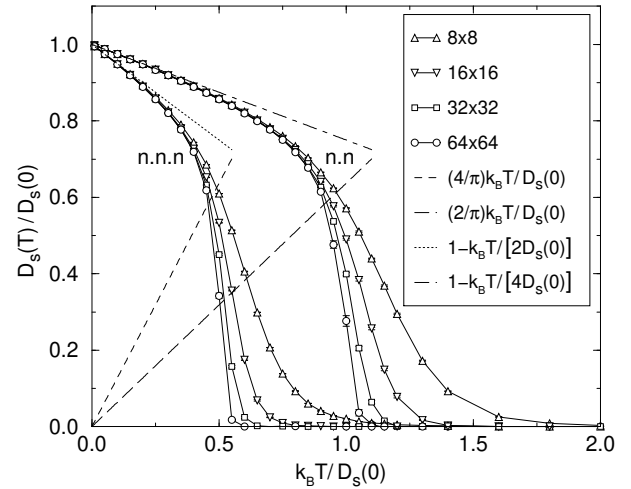


FIG. 3. Superfluid weight $D_s(T)$ vs temperature for the XY model with various lattice sizes and n.n.n or n.n interaction only. The crossings of the short (long) dashed line with the Monte Carlo data curves for the n.n.n (n.n) XY model provide estimates for the KT transition temperature T_c of increasing accuracy, as the lattice size increases. Monte Carlo points above the corresponding estimated T_c are nonzero due to finite-size effects. The dotted (dash-dotted) line depicts the low-temperature asymptote for the n.n.n (n.n) XY model, according to Eq. (A 5).

For the conventional n.n XY model it is well-known⁶ that in the thermodynamic limit we have the jump ratio: $D_s(T_c) = (k_B T_c) = 2$, or equivalently in the notation of (14), the value $R(T_c) = 1$. Hence, in view of the simple relation $D_s^{(=1)}(T) = 2D_s^{(=0)}(T)$, we anticipate for the n.n.n XY model the jump ratio: $D_s(T_c) = (k_B T_c) = 4$, or equivalently, $R(T_c) = 2$. In order to demonstrate numerically the latter property we have carried out a finite-size scaling analysis for the n.n.n XY model based on the scaling formula (14), as described in detail Sec. III. The results are summarized in Fig. 4. We note that the minimum of the $D_s^2(T)$ curve in Fig. 4(a) occurs, within numerical error, at the same point where the $R(T)$ curve in Fig. 4(b) crosses the line $R(T) = 2$. Hence the assignment $R(T_c) = 2$ leads, indeed, to a uniquely determined value for T_c which from the crossing point in Fig. 4(b) is estimated to be $k_B T_c = D_s(0) = 0.4435(5)$. The success of the finite-size scaling analysis validates then the assignment $R(T_c) = 2$ for the n.n.n XY model.

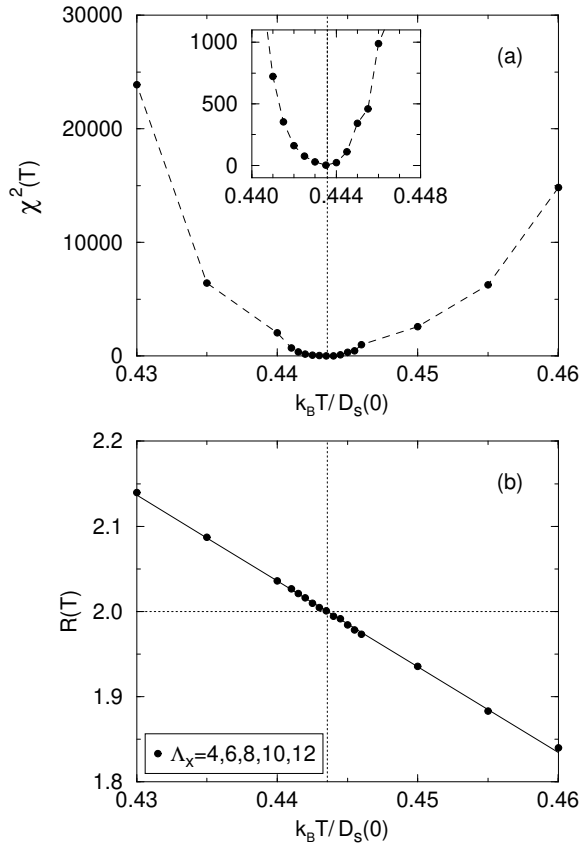


FIG. 4. Finite-size scaling around T_c for the n,n,n XY model, according to Eq. (14) and for the lattice size sequence $\Lambda_x = 4; 6; 8; 10; 12$. (a) Chi-square values (circles) of the fitting vs temperature with $R(T)$ fixed to 2. The inset is an enlarged view of the curve around its minimum. (b) Coefficient $R(T)$ vs temperature. The dotted vertical line indicates the critical temperature at which the solid line crosses the dotted horizontal line [$R(T) = 2$]. The solid line is determined by a linear fitting to the original data (circles). The estimated critical temperature is given by $k_B T_c = D_s(0) = 0.4435(5)$.

It is worth emphasizing that in terms of the dimensionless parameter $\Lambda = k_B T_c = D_s(0)$, the Monte Carlo results of the present appendix imply the value $\Lambda^{(=1)} = 0.4435(5)$ for the n,n,n XY model and, of course, twice as large corresponding value for the n,n XY model, i.e., $\Lambda^{(=0)} = 0.887(1)$. Note that the latter value for the n,n XY model agrees with the original estimate of Weber and Minnhagen¹⁹ derived with the same finite-size scaling procedure. Pictorially, our results are manifest in Fig. 3 were the crossings of the short (long) dashed line with the Monte Carlo data curves for the n,n,n (n,n) XY model provide estimates for the value of Λ of increasing accuracy, as the lattice size increases.

- ¹ A. J. M. Illis, *Nature (London)* 398, 193 (1999).
- ² Y. J. Uemura et al., *Phys. Rev. Lett.* 62, 2317 (1989); 66, 2665 (1991); *Nature (London)* 364, 605 (1993); Y. J. Uemura, *Physica C* 282-287, 194 (1997).
- ³ V. J. Emery and S. A. Kivelson, *Nature (London)* 374, 434 (1995); *Phys. Rev. Lett.* 74, 3253 (1995).
- ⁴ J. M. Kosterlitz and D. J. Thouless, *J. Phys. C* 6, 1181 (1973).
- ⁵ For reviews see, e.g., P. Minnhagen, *Rev. Mod. Phys.* 59, 1001 (1987); Z. Gulacsi and M. Gulacsi, *Adv. Phys.* 47, 1 (1998).
- ⁶ D. R. Nelson and J. M. Kosterlitz, *Phys. Rev. Lett.* 39, 1201 (1977).
- ⁷ J. Corson, R. M. Albozzi, J. Orenstein, J. N. Eckstein, and I. Bozovic, *Nature (London)* 398, 221 (1999).
- ⁸ E. Roddick and D. Stroud, *Phys. Rev. Lett.* 74, 1430 (1995).
- ⁹ M. W. Coey, *Phys. Lett. A* 200, 195 (1995).
- ¹⁰ E. W. Carlson, S. A. Kivelson, V. J. Emery, and E. Manousakis, *Phys. Rev. Lett.* 83, 612 (1999).
- ¹¹ D. A. Bonn, S. Kamal, A. Bonakdarpour, R. Liang, W. N. Hardy, C. C. Homes, D. N. Basov, and T. Timusk, *Czech. J. Phys.* 46, 3195 (1996); D. A. Bonn, S. Kamal, K. Zhang, R. Liang, and W. N. Hardy, *J. Phys. Chem. Solids* 56, 1941 (1995).
- ¹² C. Panagopoulos, B. D. Rainford, J. R. Cooper, W. Lo, J. L. Tallon, J. W. Loram, J. Betouras, Y. S. Wang, and C. W. Chu, *Phys. Rev. B* 60, 14617 (1999).
- ¹³ H. Kimura, K. Hirota, H. Matsushita, K. Yamada, Y. Endoh, S. H. Lee, C. F. Majkrzak, R. Erwin, G. Shirane, M. Grevin, Y. S. Lee, M. A. Kastner, and R. J. Birgeneau, *Phys. Rev. B* 59, 6517 (1999).
- ¹⁴ T. Suzuki, T. Goto, K. Chiba, T. Shinoda, T. Fukase, H. Kimura, K. Yamada, M. Ohashi, and Y. Yamaguchi, *Phys. Rev. B* 57, R3229 (1998).
- ¹⁵ Y. Lin, J. Sichelschmidt, J. E. Eldridge, and T. W. Ahlbrink, *Phys. Rev. B* 61, 7130 (2000).
- ¹⁶ G. C. Paltakis and N. Papanicolaou, *Phys. Rev. B* 48, 456 (1993); G. C. Paltakis, *ibid.* 51, 2979 (1995); *J. Phys. Condens. Matter* 8, 5089 (1996).
- ¹⁷ G. C. Paltakis, *J. Phys. Condens. Matter* 10, 10011 (1998).
- ¹⁸ See, for example, K. Binder and D. W. Heermann, *Monte Carlo Simulation in Statistical Physics* (Springer, Berlin, 1997).
- ¹⁹ H. Weber and P. Minnhagen, *Phys. Rev. B* 37, 5986 (1988); see also K. Harada and N. Kawashima, *J. Phys. Soc. Jpn.* 67, 2768 (1998).
- ²⁰ M. S. Hybertsen, E. B. Stechel, M. Schluter, and D. R. Jennison, *Phys. Rev. B* 41, 11068 (1990); T. Tohyama and S. Makiwawa, *J. Phys. Soc. Jpn.* 59, 1760 (1990); J. Yu and A. J. Freeman, *J. Phys. Chem. Solids* 52, 1351 (1991); T. Tohyama, C. Gazza, C. T. Shih, Y. C. Chen, T. K. Lee, S. Makiwawa, and E. Dagotto, *Phys. Rev. B* 59, R11649 (1999).
- ²¹ C. N. Yang, *Rev. Mod. Phys.* 34, 694 (1962).
- ²² M. E. Fisher, M. N. Barber, and D. Jasnow, *Phys. Rev. A* 8, 1111 (1973); J. Rudnick and D. Jasnow, *Phys. Rev. B* 16, 2032 (1977).
- ²³ D. J. Scalapino, S. R. White, and S. C. Zhang, *Phys. Rev.*

- B 47, 7995 (1993); F. F. Assaad, W. Hanke, and D. J. Scalapino, *ibid.* 50, 12835 (1994).
- ²⁴ T. T. In usk and B. Statt, *Rep. Prog. Phys.* 62, 61 (1999).
- ²⁵ A. S. Alexandrov and V. V. Kabanov, *Phys. Rev. B* 59, 13628 (1999).
- ²⁶ J. M. Kosterlitz, *J. Phys. C* 7, 1046 (1974).
- ²⁷ S. Teitel and C. Jayaprakash, *Phys. Rev. B* 27, 598 (1983).
- ²⁸ S. Lee and K.-C. Lee, *Phys. Rev. B* 49, 15184 (1994), and references therein.
- ²⁹ J. D. Jorgensen, H.-B. Schuttler, D. G. Hinks, D. W. Capone, II, K. Zhang, M. B. Brodsky, and D. J. Scalapino, *Phys. Rev. Lett.* 58, 1024 (1987).
- ³⁰ P. A. Lee and X. G. Wen, *Phys. Rev. Lett.* 78, 4111 (1997).
- ³¹ T. Xiang, C. Panagopoulos, and J. R. Cooper, *Int. J. Mod. Phys. B* 12, 1007 (1998).
- ³² A. G. Loeser, Z.-X. Shen, M. C. Schabel, C. Kim, M. Zhang, A. Kapitulnik, and P. Fournier, *Phys. Rev. B* 56, 14185 (1997); A. Kaminski, J. Mesot, H. Fretwell, J. C. Camuzano, M. R. Norman, M. Randeria, H. Ding, T. Sato, T. Takahashi, T. Mochiku, K. Kadowaki, and H. Hoehst, *Phys. Rev. Lett.* 84, 1788 (2000).
- ³³ K. Saito and M. Kaise, *Phys. Rev. B* 57, 11786 (1998).